MINERALOGICAL MAGAZINE, DECEMBER 1986, VOL. 50, PP. 693–707

A computer simulation of the structure and elastic properties of $MgSiO_3$ perovskite

A. WALL AND G. D. PRICE

Department of Geological Sciences, University College London, Gower Street, London WC1E 6BT

AND

S. C. PARKER

Department of Chemistry, University of Bath, Avon BA2 7AY

ABSTRACT. The structure and elastic properties of $MgSiO_3$, a major mantle-forming phase, have been simulated using computer models which predict the minimum energy structure by using interatomic pair potentials to describe the net forces acting between the atoms. Four such interatomic potentials were developed in this study, and are compared with potential N1 of Miyamoto and Takeda (1984). The most successful potential (W3) was derived by fitting the short range potential parameters to both the experimentally obtained structural and elastic properties of $MgSiO_3$ perovskite. The relative stabilities of some of the possible perovskite polymorphs, the orthorhombic, cubic, and tetragonal phases and hexagonal polytypes, were evaluated at 0 K and between 1 bar and 2 Mbar. The orthorhombic phase is found to be stable at all but the highest pressures, where the cubic phase may be stable. The temperature of the orthorhombic to cubic transition may decrease with increasing pressure. The energy of a stacking fault on (110) in the cubic phase was estimated using the ANNNI model and found to be about 1.95 J m^{-2} using potential W3. The distance of separation of partial dislocations of this type is predicted to increase with increasing pressure from 8.4 Å at 1 bar to 9.2 Å at 1 Mbar.

KEYWORDS: perovskite structure, $MgSiO_3$, structure simulation, mantle dynamics.

THE determination of the dynamic properties of the Earth's mantle and the way in which they relate to the processes of plate tectonics poses one of the most outstanding problems in the Earth Sciences today. Indeed, our ignorance of mantle dynamics is such that it is still considered debatable whether the mantle convects as a whole, or in layers divided by a phase or chemical change at the 670 km seismic discontinuity. At present, there are insufficient precise data available to confirm or discount either type of model. Even though it is generally accepted that magnesium silicate perovskite makes up approximately 70% of the lower mantle and 40% of the entire Earth (Poirier *et al.*, 1983), little is known about its thermal expansion behaviour, its ionic conductivity, the energetics of diffusion, or the nature of defects in the structure. All of these properties will critically influence the rheology and behaviour of the mantle. This lack of data is understandable, however, as it is not yet possible to carry out experiments to measure structural and physical properties at the high pressures and temperatures thought to characterize the lower mantle.

Most of the theories on the behaviour of mantle-forming perovskite are derived from the study of structural analogues, and the inferred bulk properties of the lower mantle. For example, O'Keeffe and Bovin (1979) and Poirier *et al.* (1983) have found that the perovskites $NaMgF_3$ and $KZnF_3$ show solid electrolyte behaviour at high temperatures, and Poirier *et al.* (1983) have also suggested that the high-temperature creep behaviour of $KZnF_3$ could be explained by a dislocation-controlled Harper–Dorn mechanism.

Work on magnesium silicate perovskite itself has mostly been confined to its synthesis, structure determinations, and study of the phase relations in the MgO–FeO–SiO_2 system. $(Mg,Fe)SiO_3$ perovskite has been synthesised by Yagi *et al.* (1978, 1982) at 400 kbars and 1000 °C, Ito and Matsui (1978) at 280 kbars and 1000 °C, and by Liu (1976) at 250 kbars and 1400 °C. However, all the structural determinations were performed at ambient conditions far removed from those actually existing in the lower mantle.

$MgSiO_3$ perovskite has an orthorhombically distorted perovskite structure with space group *Pbnm* at 25 °C and 1 bar (Liu, 1976; Ito and Matsui, 1978; and Yagi *et al.*, 1978). Yagi *et al.* (1978) found the unit cell dimensions *a*, *b*, and *c* to be 4.780, 4.933, and 6.902 Å respectively. The results from the other

studies are in close agreement. Yagi *et al.* (1982) have also investigated the structure at pressures of 74.5 kbars and 84.5 kbars, which correspond to depths in the Earth of about 220 km and 260 km. From these investigations they derived the bulk modulus (K) to be 2.6 ± 0.2 Mbar between 1 bar and 100 kbars, assuming dK/dP to be between 3 and 5. The shear modulus (μ) has not yet been evaluated experimentally although Liebermann *et al.* (1977) have estimated both the bulk modulus (2.5 ± 0.3 Mbar) and the shear modulus (1.5 ± 0.2 Mbars) on the basis of isostructural trends in compounds with the perovskite structure. As the estimated value of the bulk modulus is in good agreement with the experimental value of Yagi *et al.* (1982), we may have some confidence in the estimated value of the shear modulus of $MgSiO_3$ perovskite of 1.5 ± 0.2 Mbar. The average zero pressure thermal expansion coefficient of $Mg_{0.86}Fe_{0.14}SiO_3$ was reported by Knittle *et al.* (1986) to be 4×10^{-5} K^{-1}.

Orthorhombic perovskite (ABX_3) may be viewed as a distortion of the aristotype, cubic perovskite (Megaw, 1973). In the ideal cubic perovskite (fig. 1) the B cation is surrounded by six anions making up regular BX_6 octahedra. These octahedra share corners, creating the twelve coordinated site which is occupied by the A cation. Alternatively, the structure may be considered to have cubic close-packed AX_3 layers with the B cations occupying one quarter of the interstitial octahedral sites (those surrounded by anions only). Tilting of the BX_6 octahedra about their tetrad and diad axes (equivalent to tilting about the triad axis) reduces the symmetry from cubic to orthorhombic and the coordination of the A cations from twelve to eight (see fig. 2). The AX_8 polyhedron can be visualized as a trigonal prism capped by two additional X anions (O'Keeffe *et al.*, 1979). Other distortions of the perovskite structure (hettotypes) are well known (see, for example, Megaw, 1973; Glazer, 1975), including examples in which the B cation is displaced from the centre of the BO_6 octahedra along the tetrad axis, resulting in tetragonal symmetry as typified by $BaTiO_3$ between 0 °C and 120 °C.

Changes in pressure and temperature cause displacive phase transitions between the variants of the perovskite structure. For example, with increasing temperature, $CaTiO_3$ transforms from orthorhombic to cubic at 1260 °C (Granicher and Jakits, 1954), and $BaTiO_3$ transforms from tetragonal to cubic at 120 °C. It is, therefore, probable that $MgSiO_3$ perovskite will behave in the same way, transforming to higher symmetry at high temperatures. The effect of increasing pressure on the perovskite structure is not, however, as well known—it may decrease or increase the temperature at which a phase change to a higher symmetry perovskite may occur. Displacive phase transitions are generally rapid and nonquenchable (Hazen and Finger, 1982), and, therefore, the cubic phase of $MgSiO_3$, if it exists, is unlikely to survive in the conditions at which X-ray structure determinations have been made. In addition, it is even possible that

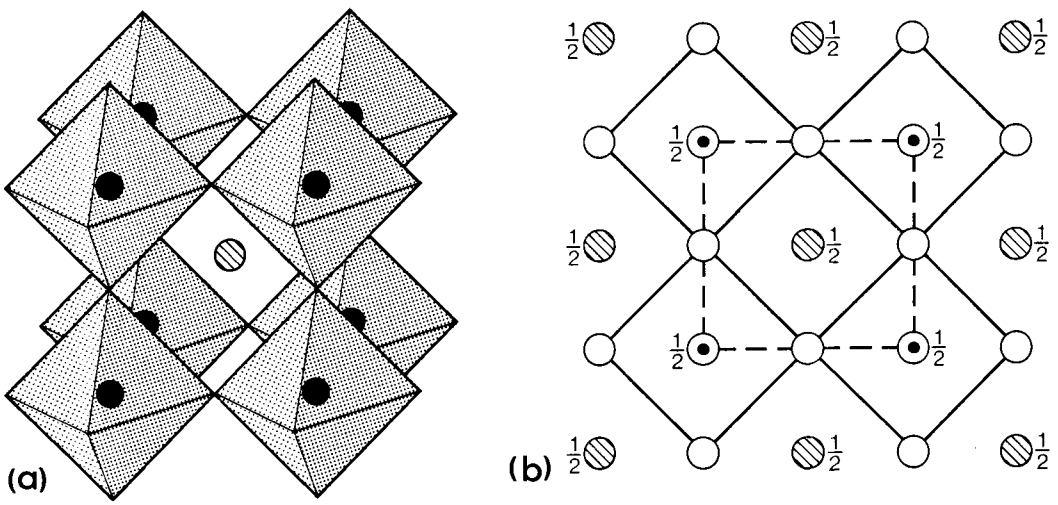

FIG. 1. The ideal perovskite structure. (*a*) Perspective view of the framework of octahedra: black circles B cations, hatched circles A cations. (*b*) Projection of the structure on to (001): the octahedra are outlined by solid lines, the unit cell by broken lines, open circles represent X anions. After Megaw (1973).

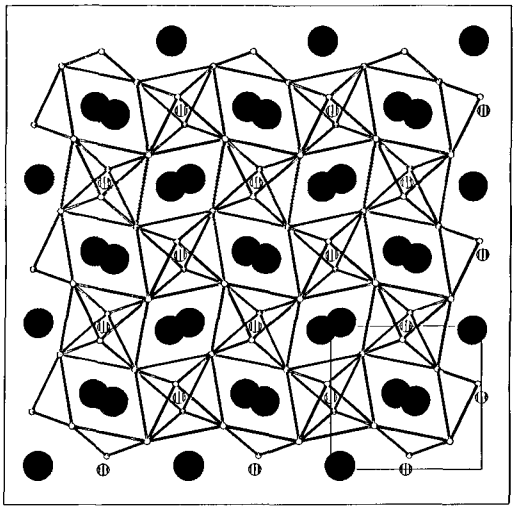

FIG. 2. Projection of the observed, distorted perovskite structure of $MgSiO_3$ on to (001): black circles Mg, hatched circles Si, open circles O. The O–O bonds in the octahedra are joined.

other perovskite-related phases, such as hexagonal perovskite polytypes, may be stable at extreme pressures far above the present experimental pressure range.

Given the experimental problems associated with studying silicate perovskites, computer simulations coupled with crystal chemical studies are the most promising source of insight into the behaviour of $(Mg,Fe)SiO_3$ perovskite. Hence, in this investigation computer modelling is used to simulate the structural and elastic properties of $MgSiO_3$ perovskite. The computer models use an atomistic approach based on the classical Born model of the solid in which potential functions represent the interactions between the atoms or ions. It has already been demonstrated that this type of computer modelling may successfully predict mineral structures and their elastic properties (for example, Parker, 1983*a*; Catlow *et al.*, 1984; Parker *et al.*, 1984; and Price and Parker, 1984). Once good potential models exist for $MgSiO_3$ perovskite, it will be possible to investigate other features of perovskite behaviour such as polytypism, defects, diffusion, phonon frequencies, and conductivity. At this preliminary stage, we only consider the end-member $MgSiO_3$ perovskite rather than the more complex, but more realistic $(Mg,Fe)SiO_3$ phase. In this study four potential models have been developed to simulate the known properties of $MgSiO_3$ perovskite at 1 bar. The results obtained using these potentials are compared with the recently published potential, N1, of Miyamoto and Takeda (1984). Three of these potentials have been used to simulate the properties of $MgSiO_3$ perovskite at high pressures which cannot readily be achieved by experiment. The relative stabilities of the cubic, orthorhombic and tetragonal perovskite polymorphs, as described above, have been evaluated and the possibility of perovskite polytypes with hexagonal packing has also been investigated. Finally we present an analysis in which the energy of a stacking fault in cubic $MgSiO_3$ perovskite is estimated using the ANNNI model approach (Price *et al.*, 1985).

Computer simulation techniques

In the atomistic approach the solid is modelled by developing interatomic potentials which describe the net forces acting upon atoms in the structure. The ability of the interatomic potentials to model the nature of interatomic forces, which may include contributions from ionic, covalent and van der Waals interactions, is crucial to the success of the simulation. The static cohesive energy of a crystal can be calculated from a summation of the interactions between the atomic pairs assuming that many-body effects are negligible. All our simulations are performed at an effective temperature of 0 K, because they do not consider the vibrational energy, and hence the static cohesive energy is equal to the total internal energy.

The computer codes WMIN (Busing, 1981) and METAPOCS (Parker, 1983*a*) use interatomic potentials to predict both the structural and elastic properties of a solid. The programs may be used in one of two modes; either to derive the potential parameters, or to find the minimum energy structure. The potential parameters may be fitted to the atomic coordinates, unit cell dimensions, and occasionally also the elastic moduli and refractive indices. Alternatively, to find the minimum energy structure resulting from specified interatomic potentials, the internal energy is minimized with respect to the coordinates of atoms in the unit cell, starting from an initial trial model which may be the experimentally determined structure.

The potential parameters used consist of two terms, a long-range electrostatic or Coulombic term and a short-range repulsive term. The electrostatic energy per formula unit is given by:

$$U_C = \tfrac{1}{2}Z \sum_{i}^{\text{one cell}} \sum_{j \neq i}^{\text{all cells}} q_i q_j r_{ij}^{-1}$$

where Z is the number of formula units per unit cell, q_i and q_j are point charges, and r_{ij} is the distance between atoms i and j. This term is slowly convergent and it is, therefore, essential that it is summed

effectively to infinity. This is achieved by using the Ewald method. Point charges are replaced by a Gaussian distribution which is transformed into reciprocal space, but the overlap between the Gaussian distributions is treated in real space. Both these terms are rapidly convergent (Catlow and Mackrodt, 1982; Parker, 1983*a*). A Born–Mayer-like expression is used to describe the short-range term:

$$U_R = \tfrac{1}{2}Z \sum_{i}^{\text{one cell}} \sum_{j \neq i}^{\text{all cells}} f(B_i + B_j) \cdot \exp[(A_i + A_j - r_{ij})/(B_i + B_j)]$$

where f is a force constant with units of energy per unit length, $A_{i,j}$ is related to the ionic radius or relative size and $B_{i,j}$ is related to the ionic compressibility. This sum is rapidly convergent and may be truncated after a suitable distance. A term representing the van der Waals interaction $(-C_{ij}r_{ij}^{-6})$ can also be included.

The shell model is an alternative to the rigid ion models described above, and provides a simple mechanical description of ionic polarizability. The atom or ion is modelled as having a core containing all the mass, surrounded by a shell of charge Y representing the outer valence electron cloud. The core and shell are coupled by a harmonic spring such that:

$$U_s(r_i) = K_i r_i^2$$

where U_s is the core-shell interaction on ion i, r_i is the core–shell separation, and K_i is the spring constant. The ionic polarizability is given by the term:

$$\alpha_i = (Y_i e)^2/K_i.$$

The METAPOCS computer code is used to calculate the elastic constants from the second derivative of the lattice energy with respect to both strain and atomic coordinates. If a shell model is used, the high frequency dielectric constant, proportional to the square of the refractive index (see, for example, Kittel, 1976), can also be calculated. Both METAPOCS and WMIN can be used to simulate the effect of pressure on a structure. In WMIN an approximation of the effect of pressure is made by introducing an extra negative energy term which is proportional to $p\Delta V$, where p is the hydrostatic pressure of interest and ΔV is the difference between the unit cell volumes at zero and the required pressure (Busing, 1981). METAPOCS has a more exact routine to simulate the effect of pressure in which the atomic coordinates are adjusted until the internal pressure is equal to the hydrostatic pressure required (Parker, 1983*b*). The internal pressure is calculated from the derivative of the lattice energy (U) with respect to the bulk strain (ε) thus:

$$P_{\text{internal}} = \partial U/\partial \varepsilon = (\partial U \cdot \partial R)/(\partial R \cdot \partial \varepsilon)$$

where R is the position of all the component vectors (coordinates and lattice parameters). The results from WMIN and METAPOCS are similar for low pressures but differ by up to 4% at 2 Mbars.

The short-range potential parameters may be derived empirically by fitting them to experimentally determined data, or non-empirically either using Hartree–Fock molecular orbital methods which are expensive in computer time, or the more computationally economic electron gas method based on a statistical atom model (Catlow and Mackrodt, 1982). In this study four potentials W1, W2, W3, and W4 (Table I) were derived by fitting the potential parameters to the experimentally determined data for $MgSiO_3$ perovskite, although the $O^- \ldots O^-$ short-range term in W4 was derived using the Hartree–Fock method. These potentials are compared with potential N1 of Miyamoto and Takeda (1984) which was derived by fitting to the Mg_2SiO_4 olivine structure rather than to $MgSiO_3$ perovskite.

Table I The potential parameters.

	A_{Mg}	A_{Si}	A_O	B_{Mg}	B_{Si}	B_O
W1	1.1731	1.9410	1.6221	0.0450	0.1800	0.1291
W2	1.1419	1.9400	1.6175	0.0204	0.2019	0.1469
W3	1.0876	1.7732	1.7069	0.0238	0.1757	0.1503
W4	2.2389	2.6065	1.1230	0.2170	0.2579	0.0745
N1	0.97	0.608	1.770	0.065	0.0172	0.105

W1. To derive this potential WMIN was used to fit the potential parameters to the X-ray data for $MgSiO_3$ perovskite from Yagi *et al.* (1982). Full ionic charges of Mg +2.0, Si +4.0, and O −2.0 were assumed.

W2. This derivation of this potential was similar to that of W1, WMIN being used to fit the potentials to X-ray data, but the oxygen and silicon charges were varied by trial and error until a reasonable prediction of the bulk modulus was achieved. The optimum partial charges were found to be Mg +2.0, Si +2.8, and O −1.6.

W3. This potential includes a shell model for oxygen to simulate its ionic polarizability. Using METAPOCS the potential parameters were fitted to X-ray data, bulk and shear moduli, and a calculated refractive index. The ionic charges in the potential thus developed were Mg +1.899, Si +3.168, O core +0.201, and O shell −1.889 with a spring constant of 81.71 $kJ^{-2}\ mol^{-1}$.

The refractive index of $MgSiO_3$ perovskite has not been measured experimentally. Instead we used a calculated value of 1.839 ± 0.004, which was

obtained using the Gladstone–Dale relationship between refractive index, chemical composition, and density described by Mandarino (1976, 1978, 1979). To assess the accuracy of this method when applied to perovskites, calculations were made for $CaTiO_3$, $SmTiO_3$, $GdAlO_3$, and $ScAlO_3$. Their measured mean refractive indices are 2.318, 2.052, 2.014, and 1.94 respectively (the latter three values are from Bass, 1984). The values calculated using the Gladstone–Dale relationship are 2.284, 2.058, 2.053, and 2.010. The small differences, all less than 0.07, between the calculated and measured refractive indices demonstrate that it is reasonable to use this method for perovskites.

W4. In this potential the values for the $O^- \ldots O^-$ short-range term were taken from Catlow (1977), and were derived using Hartree–Fock methods. An empirically derived value for the van der Waals coefficient between $O^{2-} \ldots O^{2-}$ of 2690 kJ Å^6 mol^{-1} was also included. The remaining Mg–O and Si–O short-range terms were fitted to the structural data of Yagi *et al.* (1982). Full ionic charges were used.

N1. This potential was developed by Miyamoto and Takeda (1984) who used WMIN to fit the potential parameters to the structural data of Mg_2SiO_4, starting with values of A_{Mg} and B_{Mg} obtained by fitting to $MgCl_2$. Again full ionic charges were used.

Silicates are known not to be fully ionic in character and, therefore, partially ionic charges were introduced into potentials W2 and W3 with the aim of improving the nature of the simulated Si–O bond. Price and Parker (1984) successfully used a Morse potential to model the covalency of the Si–O bond in olivine, in which Si has tetrahedral coordination. However, fitting a Morse potential to the Si–O bond in $MgSiO_3$ perovskite failed, probably because SiO_6 octahedra have less covalent character than SiO_4 tetrahedra. Swanson and Prewitt (1983) demonstrated that this is, indeed, likely to be the case by their detailed electron density study of $K_2Si^{VI}Si^{IV}O_9$, from which they inferred that the partial ionic charges on Si^{VI}, Si^{IV}, and O are +3.29(15), +2.52(11), and −1.43(8) respectively. The Si^{VI} charge of +3.168 in potential W3 and that reported by Swanson and Prewitt (1983) agree within the error of their determination, although the charge of +2.8 in W2 is slightly lower.

The purely empirically derived potentials W1, W2, and W3 have similar *A* (relative ionic radius) and *B* (relative ionic compressibility) parameters. However, this is not the case for the potentials which include terms transferred from other compounds, W4 and N1. The B_{Si} and B_{Mg} values are larger in W4 than in the totally fitted potentials and the B_O value is smaller, giving a structure with comparatively soft cations and rigid anions in accord with the observations made by Prewitt (1985). In N1, the magnesium ion is relatively more compressible, but the silicon and oxygen ions are more rigid than in the empirically derived potentials.

The extent to which these potentials can be used to reproduce the experimentally determined structural and elastic properties of $MgSiO_3$ perovskite will be discussed in the following section. In subsequent sections the potentials will be used to predict the structure of $MgSiO_3$ at pressures of up to 2 Mbars, and to investigate the behaviour of phases structurally related to orthorhombic perovskite.

Comparison of the experimental and simulated results

The success with which the five potentials W1, W2, W3, W4, and N1 simulate $MgSiO_3$ perovskite at 1 bar can be assessed from the results presented in Table II. As would be expected, the structures simulated using the three empirically derived potentials, W1, W2, and W3 are in good agreement with that determined experimentally. Of these potentials, the best reproduction of the unit cell dimensions *a*, *b*, and *c* is achieved using W1, with a root mean squared (rms) error of only 0.018 Å. Potentials W1 and W3 give the best prediction of Si–O bond lengths (the rms errors are less than 0.013 Å). The variation of bond lengths within the SiO_6 octahedron provides a measure of its distortion. This is best reproduced using W2 and W3, while W1 predicts an octahedron which is too regular. The Mg–O bond lengths are predicted well by W3 (rms error of 0.029 Å). W2 also reproduces the Mg–O lengths well (the rms error for the shortest six bonds is 0.026 Å), but it overestimates the longest Mg–O bonds by 0.1 Å giving an overall rms error of 0.055 Å. The elastic moduli are not so well reproduced. The fully ionic potential, W1, predicts shear and bulk moduli that are too stiff by a factor of 1.7 and in contrast, the moduli from W2 are a factor of 0.7 too soft. The values from W3, which was fitted to elastic data, are good, being within the error of the experimental values and those predicted by Liebermann *et al.* (1977).

Potentials W4 and N1, which were not entirely derived by fitting to perovskite data, also produce reasonable results. The unit cell dimensions are reproduced well by W4 (rms error of 0.033 Å), but N1 produces unit cell dimensions that are too large with a rms error of 0.130 Å. The rms errors in the Si–O bond lengths of 0.029 Å from W4 and 0.045 Å from N1 are both larger than for W1, W2, or W3,

Table II. Comparison of the simulated and experimentally determined unit cell parameters

	Experimental*	W1	W2	W3	W4	N1
a(Å)	4.780	4.785	4.775	4.979	4.802	4.862
b(Å)	4.933	4.925	4.931	4.949	4.884	5.043
c(Å)	6.902	6.932	7.021	6.957	6.881	7.084
V(Å^3)	162.747	163.365	163.315	165.162	161.379	173.693
I(Å)**		0.018	0.069	0.023	0.033	0.130
Si-O2(2)	1.760	1.782	1.782	1.767	1.762	1.824
Si-O1(2)	1.819	1.815	1.845	1.808	1.776	1.848
Si-O2(2)	1.789	1.783	1.768	1.797	1.764	1.824
I(Å)**		0.013	0.020	0.013	0.029	0.045
Mg-O2(2)	2.064	2.051	2.072	2.097	2.049	2.029
Mg-O1(1)	2.099	2.203	2.034	2.061	2.026	1.981
Mg-O1(1)	2.124	2.115	2.089	2.130	2.228	2.325
Mg-O2(2)	2.194	2.246	2.180	2.247	2.377	2.431
Mg-O2(2)	2.473	2.506	2.573	2.493	2.448	2.526
I(Å)**		0.041	0.055	0.029	0.119	0.171
K(Mbar)	2.62	4.38	2.08	2.58	3.32	7.14
μ(Mbar)	1.50	2.53	1.07	1.33	1.98	4.35

* Yagi et al.(1982)

** $I = (\Sigma((d_{obs}-d_{calc})^2/n))^{1/2}$

and the predicted SiO_6 octahedra are too regular. Potentials W4 and N1 do not reproduce the Mg–O bond lengths as well as W1, W2, and W3, giving comparatively large errors of 0.119 Å (W4) and 0.171 Å (N1). Like the other fully ionic potential W1, the predicted bulk modulus values for W4 and N1 are too stiff by factors of 1.3 and 2.7 respectively (see Table II).

It can be concluded, therefore, that the simulations of $MgSiO_3$ perovskite using the transfer potentials W4 and N1 are not as successful as those achieved using the empirical potentials fitted entirely to perovskite data (W1, W2, and W3). In particular, they are less capable of predicting the Mg–O or Si–O bond lengths. Simulation of $MgSiO_3$ perovskite at higher pressures has, therefore, been confined to using potentials W1, W2, and W3.

A comparison of the simulated and experimentally determined structure of $MgSiO_3$ perovskite (from Yagi *et al.*, 1982) at pressures of 74.5 kbar and 84.5 kbar is shown in fig. 3. All the calculated unit cell lengths are within 1% of those determined experimentally.

The change in unit cell volume with increasing pressure (fig. 3) is best reproduced by W3; this is reflected in the calculated bulk modulus (K). The values of dK/dP obtained using W1, W2, W3 are 3, 5, and 5 respectively—all within the range of 3 to 5 assumed by Yagi *et al.* (1982). However, only the bulk modulus values of W2 (2.08–2.55 Mbar) and W3 (2.55–3.04 Mbar) are close to the experimentally determined value of 2.6 Mbars between 0 and 100 kbar. The shear moduli (μ) predicted by W1, W2, and W3 between 0 and 100 kbar, are 2.5 to 2.7 Mbar; 1.1 to 1.3 Mbar; and 1.3 to 1.6 Mbar respectively. When compared with the inferred value of the shear modulus of 1.5 ± 0.2 Mbars (Liebermann *et al.*, 1977), it is again found that the values from W1 are too stiff, while those from W2 are too soft, and that only those from W3 are in good agreement. The pressure dependence of the shear modulus, $d\mu/dP$, predicted by W2 and W3 is similar (2.7 and 2.8), and that of W1 is slightly lower (1.46).

The ratios of the unit cell parameters a, b, and c can be used to investigate any change in the orthorhombic distortion of $MgSiO_3$ perovskite

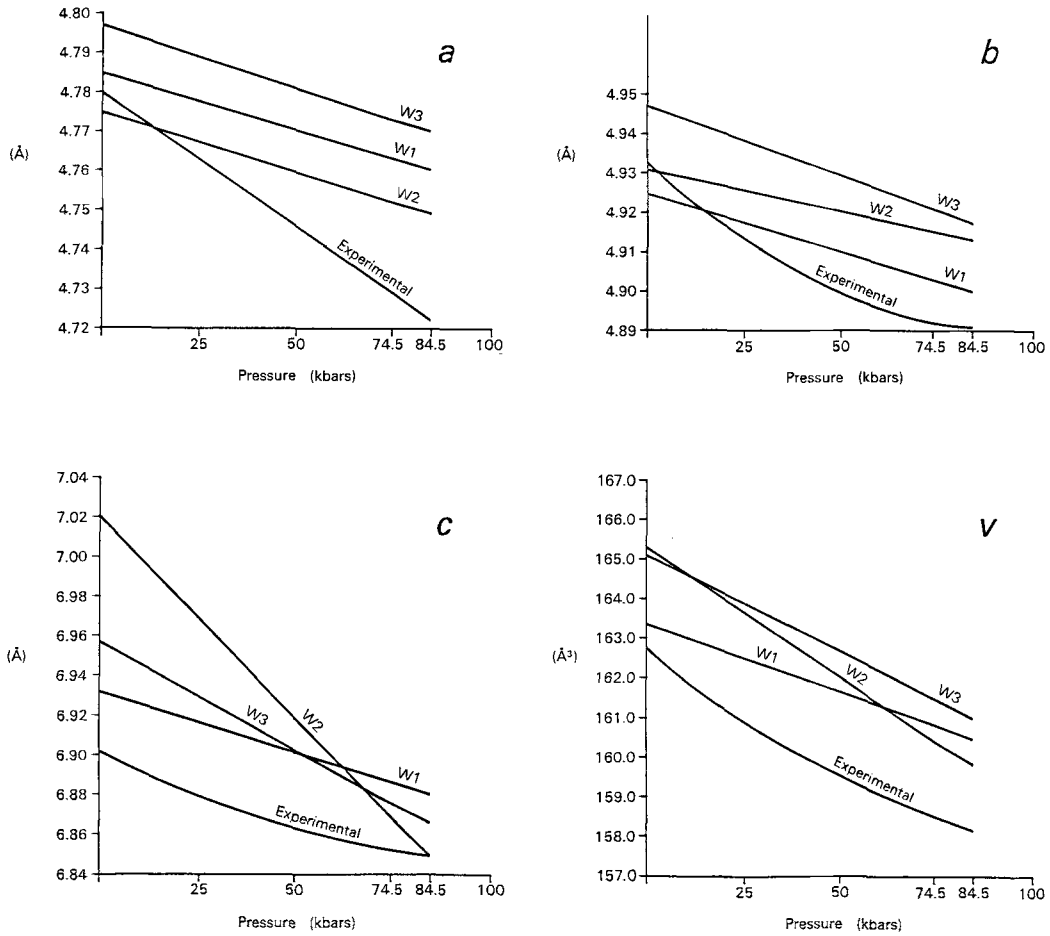

FIG. 3. Comparison of the simulated and experimentally determined unit cell parameters a, b, c, and V for orthorhombic $MgSiO_3$ perovskite.

with increasing pressure. If the distortion becomes less, the ratios will tend towards those of the ideal cubic perovskite, which are $b/a = 1{\cdot}0$ and $c/a = c/b = \sqrt{2}$. Over this pressure range the ratios show no clear trends. Potentials W1, W2, and W3 predict similar results in that the c/a ratios become closer to $\sqrt{2}$, the c/b ratios deviate from $\sqrt{2}$, and the b/a ratios either stay about the same or trend away from 1. Yagi *et al.* (1978) found that the c/b ratio tends towards $\sqrt{2}$ with increasing pressure, but the b/a and c/a ratios do not approach the ideal values.

As the elastic properties of a mineral are more difficult to simulate than its structure, they provide a more rigorous test of the suitability of a potential (Burnham, 1985). This is because they depend on the second derivative of the potential function, whereas the structural parameters depend only on the first. The three fully ionic models all give elastic moduli that are too rigid. An improved model is obtained with the partial charges of W2 and good results from the shell model, W3. Therefore, we conclude that W3 is the most useful potential yet developed to describe $MgSiO_3$ perovskite, as it reproduces well both the structural and elastic properties of this major Earth-forming mineral.

The effect of pressure on the orthorhombic, cubic, and tetragonal perovskite polymorphs and phase transitions between them

Changes in the perovskite structure at depth in the Earth may influence the rheology of the mantle. To investigate the nature and possibility of any

structural alterations, we have simulated the observed orthorhombic, and hypothetical cubic, and tetragonal polymorphs of $MgSiO_3$ perovskite, described above, at pressures of 0 kbar, 100 kbar(10 GPa), 200 kbar(20 GPa), 500 kbar(50 GPa), 1 Mbar(100 GPa), and 2 Mbar(200 GPa), corresponding to depths in the Earth of approximately 300 km, 600 km, 1270 km, 2270 km, and 3470 km according to the Preliminary Reference Earth Model (Dziewonski and Anderson, 1981). At any given pressure and temperature, only one of these possible polymorphs can be stable. Changes in pressure and/or temperature may, however, cause one polymorph to transform to another. The Gibbs free energies (G) of the various possible perovskite polymorphs were calculated at zero temperature and the pressures of interest, to provide a measure of their relative stability. Phase transitions between these perovskite polymorphs are displacive and may be of first or higher order. We, therefore, also investigated changes in the distortion of the tetragonal and orthorhombic perovskite polymorphs with increasing pressure to see whether continuous (or second order) phase transitions were predicted to occur.

Computer simulation results. The Gibbs free energy (G) was derived using the relationship $G = U + P \cdot V - T \cdot S$, where U is the calculated lattice energy, P is the pressure of interest, V is the molar volume, T the temperature and S the entopy. As the simulations are effectively at absolute zero, the product $T \cdot S$ is also zero. Evaluation of the free energy shows that at 1 bar, in agreement with the observed behaviour of $MgSiO_3$ perovskite, the orthorhombic polymorph is the more stable form, irrespective of the potential used (whether W1, W2, or W3). It was also found that the tetragonal polymorph was predicted to have a stability intermediate between that of the orthorhombic and cubic phases. At higher pressures the relative free energies and the predicted changes in structural distortion of the polymorphs differ according to the potential used. Potential W1 predicts that the orthorhombic phase is always more stable than the cubic, with the difference in their free energy (ΔG) increasing with increasing pressure (see fig. 4 and Table III*a*). In contrast, W2 and W3 predict that the difference in free energy between the two phases becomes less at higher pressure (fig. 4, Table III*a*). By 2 Mbar both W2 and W3 predict that the cubic phase is the more stable.

In addition to different energetic behaviour, our simulations of the structure of orthorhombic $MgSiO_3$ perovskite show that the changes in the orthorhombic distortion as a function of pressure also vary according to the potential used. All three potentials predict a decrease in a, b, c, and V with

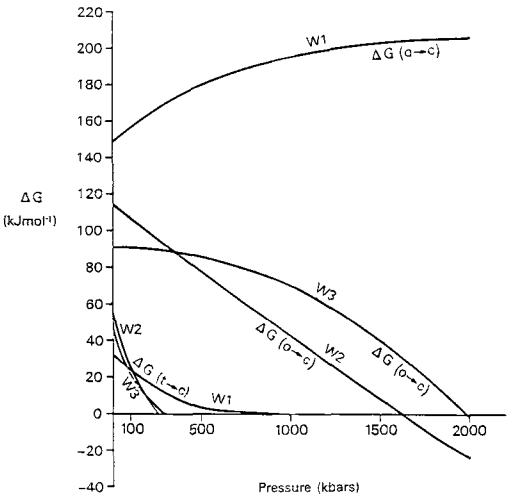

FIG. 4. Comparison of the Free energy difference ΔG between the orthorhombic and cubic phases ($\Delta G(o-c)$), and the cubic and tetragonal phases ($\Delta G(t-c)$).

increasing pressure. However, the extent of the change is different for each potential (see fig. 5). W1 predicts the least contraction of the unit cell and W2 the most, in accordance with their calculated bulk moduli. The ratios between a, b, and c predicted by W1 deviate from the ideal cubic values whilst, in contrast, those from W2 and, to a lesser extent from W3, become closer to them. An alternative way of looking at the degree of orthorhombic distortion of $MgSiO_3$ perovskite is to consider the rotation of the SiO_6 polyhedron about its threefold axis. This angle of rotation φ can be calculated using the relationship developed by O'Keeffe *et al.*,

Table IIIa Calalculated ΔG ($kJmol^{-1}$) for the orthorhombic to cubic perovskite phase transition.

P(kbar)	0	100	200	500	1000	2000
W1	148.4	156.4	163.6	179.8	195.7	205.8
W2	114.6	106.8	93.8	78.3	42.5	-24.0
W3	91.2	91.2	86.1	86.1	71.5	-1.1

Table IIIb Calculated ΔG ($kJmol^{-1}$) for the tetragonal to cubic perovskite phase transition.

P(kbar)	0	100	200	500	1000	2000
W1	31.9	22.9	15.9	3.4	0.1	-1.1
W2	56.6	25.4	5.1	-0.4	-0.4	0.7
W3	47.7	21.8	4.0	-0.0	0.0	-0.0

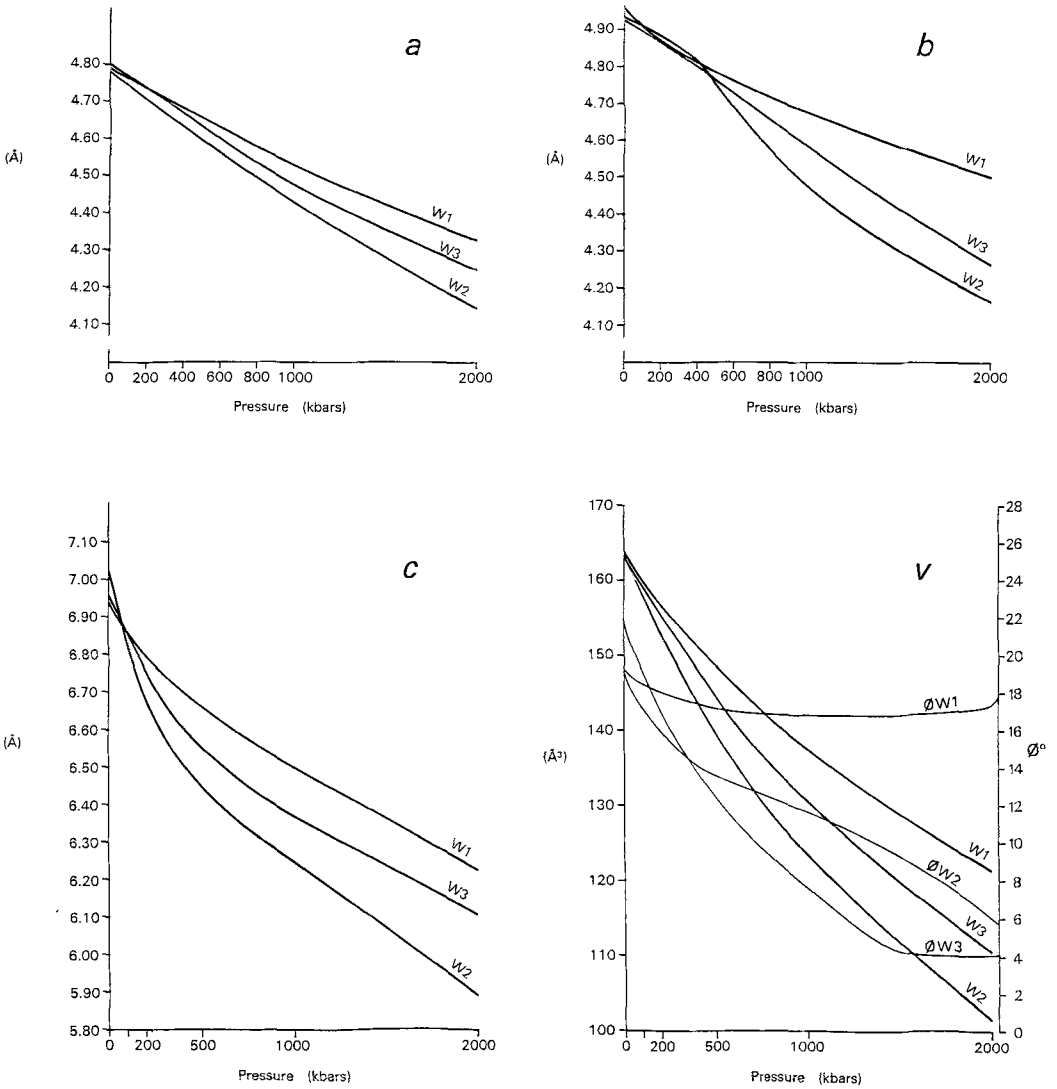

FIG. 5. Comparison of the unit cell parameters a, b, c, and V, and the angle of rotation, φ, of the SiO_6 octahedron about the threefold axis for orthorhombic perovskite simulated using potentials W1, W2, and W3 between 0 and 2 Mbars pressure.

1979 (which applies strictly to regular octahedra) of $\varphi = \cos^{-1}(\sqrt{2a^2}/bc)$ (where we use a, b, c as defined by Yagi *et al.*, 1978, not O'Keefe *et al.*, 1979). Perovskite with an ideal cubic structure has a φ value of zero degrees. The results from W2 and W3 show a decrease in φ between 0 Mbar and 2 Mbar of 22° to 4° and 19° to 6° respectively (see fig. 5) and, therefore, also a decrease in orthorhombic distortion with increasing pressure. These results suggest that because the value of φ has not decreased to 0 by 2 Mbars, the phase transition, predicted by calculation of the free energy, would be of first order. In contrast the value from W1 changes little from 18°.

The free energy difference between the metastable tetragonal and cubic phases ($\Delta G(t-c)$) calculated for all three potentials is predicted to gradually decrease to zero with increasing pressure (see fig. 4 and Table III*b*). This occurs at about 300 kbar using W2, 350 kbar using W3, and above 500

kbar using W1. The unit cell dimensions of the tetragonal phase also gradually become closer to those of the simulated cubic perovskite and they are actually equal at the pressures above the inversion pressure ($\Delta G = 0$). Our computer simulations using potentials W1, W2, and W3, therefore, predict that a phase transformation, possibly second order, occurs between the hypothetical tetragonal and cubic phases with increasing pressure.

In an attempt to determine which potential provides the best model of $MgSiO_3$ perovskite behaviour in response to increasing pressure, we will look at the results of some experimental studies on the effects of pressure on phase transitions in perovskites, and also at some possible crystal chemical approaches to the problem.

Experimental studies on perovskites. The small number of experimental studies of the effects of hydrostatic pressure on phase transitions between perovskite polymorphs show that, at least within the pressure range investigated (0 to 60 kbars), perovskite phase transitions may have a negative or positive dP/dT slope. For example, phase transitions between the orthorhombic and rhombohedral polymorphs of $BaTiO_3$ (Samara, 1971); the tetragonal and cubic polymorphs of $BaTiO_3$ (Clarke and Benguigui, 1977); the orthorhombic and pseudocubic monoclinic polymorphs of $CdTiO_3$ (Martin and Hegenbarth, 1973); and the tetragonal and cubic polymorphs of $PbTiO_3$ (Ikeda, 1975) have a boundary between the two phases with a negative dP/dT slope—the phase change being caused by both increasing pressure and temperature. The dP/dT slope has been found experimentally to be positive for the phase changes between orthorhombic and cubic $PbZrO_3$ (Samara, 1970); orthorhombic and cubic $PbHfO_3$ (Samara, 1970); tetragonal and cubic $SrTiO_3$ (Okai and Yoshimoto, 1975); and tetragonal and cubic $KMnF_3$ (Olai and Yoshimoto, 1975). Only the distortions in $SrTiO_3$ and $KMnF_3$ are caused by rotation of the BX_6 octahedra (in this case about the tetrad axis); the others are caused by displacement of the B cations from the centres of the octahedra. All these phase transitions are first order except those in $BaTiO_3$, $PbZrO_3$, and $PbHfO_3$ at high pressure which are second order. Thus the behaviour of $MgSiO_3$ perovskite is not obviously predicted from these experimental results.

Crystal chemical arguments. A crystal chemical approach to the study of the effect of pressure on the degree of orthorhombic distortion in $MgSiO_3$ perovskite was used by Yagi *et al.* (1978) and O'Keeffe *et al.* (1979), with conflicting results. Yagi *et al.* (1978) developed a relationship between the degree of orthorhombic distortion, the relative sizes of BX_6 octahedra and the A cation in the perovskite structure (ABX_3) using their ionic radii in octahedral coordination (although Mg has a coordination number of at least 8). They predicted that the structure would become more regular at high pressures. O'Keeffe *et al.* (1979) arrived at the opposite conclusion by deriving a relationship for the change in φ, the angle of rotation of the SiO_6 octahedron about its threefold axis, in terms of the relative compressibilities of the A–X (l) and B–X (L) bonds: $(d\cos\varphi/dP) = (x/2)(\beta l - \beta L)\cos\varphi$, where $x = 0.854$ (Yagi *et al.*, 1978). A positive change in φ indicates an increase in distortion and, conversely, a negative change a decrease. They predicted a rate of change in φ of 1° per 100 kbars using the structure of $MgSiO_3$ determined by Yagi *et al.* (1978). However, their conclusion is not very reliable because the value of βL used was taken from Mg–O bonds in octahedral coordination in garnet between 1 bar and 60 kbar, whereas the Mg^{2+} in perovskite has a coordination number of at least 8. In addition, βl was calculated by assuming it to have half the compressibility of βL. Our computer simulations show that this is unlikely to be true, particularly for the shortest six Mg–O bonds.

Changes in the overall structure of $MgSiO_3$ perovskite will almost certainly be determined by the relative compressibilities of the constituent MgO_8 and SiO_6 polyhedra, so it is important that these are modelled well. The calculated SiO_6 polyhedral bulk modulus in perovskite may be compared with that of stishovite (made up of SiO_6 polyhedra) provided that the polyhedral bulk modulus is independent of the structure (Hazen and Finger, 1982). To calculate the polyhedral bulk modulus, the SiO_6 octahedra are assumed to be regular, allowing the mean bond length to be used. The calculated bulk modulus values are 7.4 Mbar from W1, 2.1 Mbar from W2 and 3.0 Mbar from W3. The experimentally determined value for SiO_6 in stishovite is 3.5 ± 1.5 Mbar (Hazen and Finger, 1982), again demonstrating that W1 predicts a bulk modulus value that is much too high, whereas W2 gives one which is too low, but just on the limit of the estimated error. W3 produces the best model of the SiO_6 polyhedra, particularly as it has been shown above to reproduce the Si–O bond lengths well. The linear compressibilities of the six Mg–O bonds in the trigonal prism and of the two longer bonds outside the prism have also been calculated. As would be expected, the shorter bonds are less compressible than the longer ones. Potential W2 generates the least compressible short bonds and the most compressible long ones; their compressibilities differ by a factor of thirty-one. This would contribute to the increased regularity in bond lengths predicted at high pressures. W1 has

the opposite effect, giving the most compressible short bonds and the most rigid long bonds differing by a factor of two only. The shape of the MgO_8 polyhedron is, therefore, less likely to vary with increasing pressure. W3 lies between the other two, the long bonds being five times more compressible than the short ones.

Using the relationship between cell volume and φ given by O'Keeffe *et al.* (1979), we have developed the following relationship between the change in φ with pressure, the bulk modulus of the SiO_6 polyhedra, K_{SiO_6}, and the total bulk modulus K_{pv}:

$$d\varphi/dP = \tfrac{1}{2}\cot\varphi(1/K_{pv} - 1/K_{SiO_6}),$$

and hence avoided direct consideration of the compressibility of the ill-defined Mg–O polyhedra. With 18° as the value of φ at 1 bar (Yagi *et al.*, 1978), 2.6 Mbar for K_{pv} (Yagi *et al.*, 1982) and 3.5 Mbar for K_{SiO_6} derived from stishovite, $d\varphi/dP$ is found to be 8.7° $Mbar^{-1}$. However, the errors in the determination of both bulk moduli are such that this value could be positive or negative—the degree of distortion at 1 bar may be increasing or decreasing. Using the φ values and bulk moduli predicted by potentials W1, W2, and W3 results in $d\varphi/dP$ values of 8.0° $Mbar^{-1}$, −0.4° $Mbar^{-1}$, and 4.5° $Mbar^{-1}$ respectively. This relationship predicts a positive change in φ if K_{pv} is smaller than K_{SiO_6} and, therefore, the pressure dependence of the bulk moduli is important in determining $d\varphi/dP$ at high pressure. For example, at 1 Mbar the simulated K_{pv} is 8.8 Mbar, 6.0 Mbar, and 7.06 Mbar and K_{SiO_6} about 9.5 Mbar, 4.8 Mbar, and 6.1 Mbar using W1, W2, and W3 respectively and results in $d\varphi/dP$ values of 0.7° $Mbar^{-1}$, −9.3° $Mbar^{-1}$, and −3.0° $Mbar^{-1}$. Hence it is possible that, although the distortion is predicted to increase at low pressure, it actually decreases at high pressure as the relative magnitudes of the polyhedral bulk moduli alter. Obviously more extensive experimental studies are required to investigate this possibility.

In conclusion, the experimental results on other perovskites and the results from computer simulation of the metastable tetragonal to cubic phase transition agree well; the transition is predicted to have a negative dP/dT slope and would probably be of second order at high pressure. The results for the orthorhombic to cubic transition are not so clear. Some of the experimental results, including those of Yagi *et al.* (1982), and the prediction of O'Keeffe *et al.* (1979) based on crystal chemical relationships, suggest that the transition has a positive dP/dT slope (assuming that the effect of increasing the temperature is to increase the structural symmetry), but computer simulations using W2 and W3 predict a negative dP/dT slope. However, the experimental results and the relationship of O'Keeffe *et al.* (1979) are only derived at relatively low pressures (all less than 100 kbars). As argued above, it is possible that the distortion of the perovskite structure with increasing pressure could reach some maximum value before the structure starts to become closer to that of the ideal cubic perovskite. Potential W3, which best models $MgSiO_3$ perovskite, predicts such behaviour with $d\varphi/dP$ being greater than 0 at low pressures, but less than 0 at high pressures of the order of 1 Mbar. However, this potential predicts that the cubic perovskite phase becomes stable with respect to the orthorhombic phase before φ reaches 0, therefore, suggesting that at 0 K at least, any phase transition between these phases would be of first order. These results highlight the need for more experimental studies to determine the existence and nature of any phase transitions between different perovskite structures in the Earth's mantle.

Simulation of perovskite polytypes and the calculation of stacking fault energies

The perovskite structure is highly versatile because, besides the various distortions described above, it can also give rise to a number of stacking variants resulting in perovskite polytypes. Most notable of these are the hexagonal perovskites (see for example, Muller and Roy, 1974) in which variations in the stacking of the close-packed AX_3 layers produce a hexagonal rather than a cubic cell. It is also possible to define layers on {110} of the cubic perovskite which can be stacked in one of two ways to produce a series of hypothetical perovskite polytypes. Isolated defects related to these polytypic modifications may feature in the deformation of mantle-forming perovskite, or they may even occur as high-pressure stable modifications of the known perovskite structures. We have used some of the potentials developed in the previous sections to investigate these possibilities and to estimate the energetics of isolated (110) planar defects in cubic perovskite.

Hexagonal polytypes. Hexagonal perovskites form equilibrium phases for several transition-metal-bearing perovskites, including for example $BaNiO_3$, $BaMnO_3$, and $BaTiO_3$ (Muller and Roy, 1974). The ideal cubic perovskite can be considered as being composed of close packed AX_3 layers arranged in a cubic close packed sequence repeating every three layers. In contrast, the completely hexagonally close packed structure, based on $BaNiO_3$, has a two layer repeat. In the hexagonal form, each BX_6 octahedron shares two opposite faces with its neighbours, giving a one dimensional octahedral chain along the hexagonal c axis. In our simulation we modelled the four relatively common

Table IV Free energies ($kJmol^{-1}$) of the hexagonal and cubic polytypes of $MgSiO_3$ perovskite.

P(kbar)	$[SrTiO_3]$	$[BaTiO_3]$	$[BaMnO_3]$	$[BaNiO_3]$
0*	-9995.5	-10028.8	-9889.9	-9647.8
500	-8885.2	-8839.8	-8711.1	-8380.0
1000	-7894.1	-7811.7	-7689.4	-7298.7
2000	-6113.8	-5992.8	-5873.4	-5402.1

*The orthorhombic phase has the lowest energy of $-10109.6 kJmol^{-1}$.

polytypes, the ideal cubic structure (as in $SrTiO_3$ at ambient conditions), the hexagonal structure (exhibited by $BaNiO_3$), and two structures with mixed cubic and hexagonal packing sequences based on $BaMnO_3$ and hexagonal $BaTiO_3$. These hypothetical $MgSiO_3$ perovskite polytypes were simulated at pressures of 0 to 2000 kbars using potential W2, and their free energies calculated (see Table IV) to provide a measure of their relative stabilities. We found that the introduction of hexagonal packing destabilizes the perovskite structure, particularly at high pressure, and that polytypes with the most hexagonal stacking sequences were the least stable

$$([BaNiO_3] < [BaMnO_3] < [BaTiO_3] < [SrTiO_3]).$$

Therefore, hexagonal $MgSiO_3$ perovskites seem unlikely to occur as mantle-forming phases.

{110} *polytypes.* After an experimental study of $KZnF_3$ (which has the cubic perovskite structure), Poirier *et al.* (1983) suggested that one of the active slip systems may have had dislocations with a Burgers vector [110] able to glide on (110) planes. In this case, splitting of the type:

$$[110] = \tfrac{1}{2}[110] + \tfrac{1}{2}[110]$$

would result in a stacking fault on the (110) plane. The fault leaves the anion sublattice unaltered, but forms edge-sharing octahedra in which the distances between both the A and B cations is shortened to $a/\sqrt{2}$.

The cubic perovskite structure of $MgSiO_3$ can be considered to be made up of structural units related to each other by a glide operator $\frac{1}{2}[110]$ (110). If the basic structural unit (fig. 6) is represented by ↑, the sequence of units in the ⟨110⟩ direction is ↑↓↑↓↑↓ or ⟨1⟩, representing a series of units effectively stacked in alternate directions. An infinite number of sequences are possible; for example a sequence ↑↑↓↑↑↓ would be denoted as ⟨21⟩ and can be described as being made up of one band of two arrows and one band of one arrow (Fisher and Selke, 1981). More generally, $\langle n_1, n_2, \ldots, n_m \rangle$ denotes a structure made up of m bands of arrows or structural units of length $n_1 n_2, \ldots, n_m$. The occurrence of a stacking fault on {110} in the ideal cubic (⟨1⟩) structure, which places two structural unit stacked in the same orientation adjacent to each other, will alter the sequence to ↑↓↑↑↓↑.

Now that potential models have been developed to describe the $MgSiO_3$ perovskite structure, it is possible to evaluate the energy of this stacking fault using the ANNNI (Axial Next Nearest Neighbour

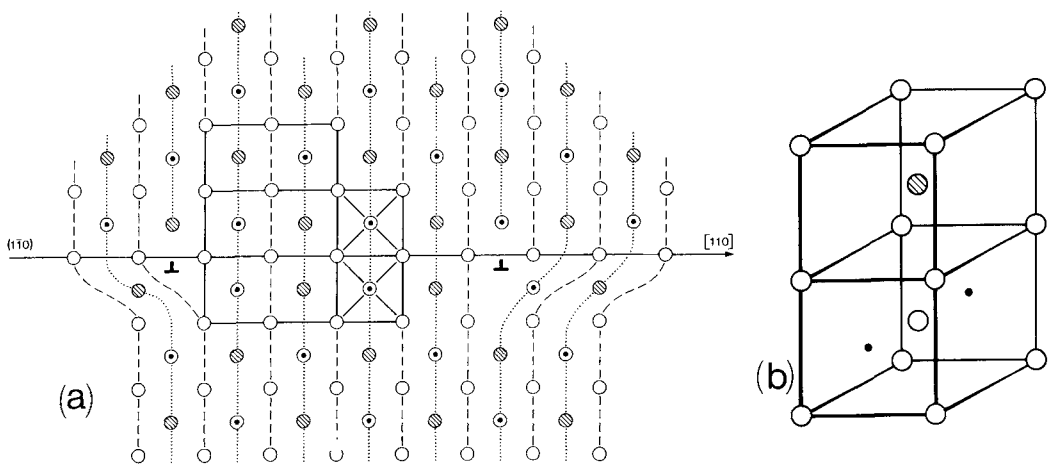

FIG. 6. (*a*) Split ⟨110⟩ edge dislocation on a {110} plane: black circles Si, hatched circles Mg, open circles O. Two edge sharing octahedra are outlined across the stacking fault, together with three stacking units parallel to the fault. After Poirier *et al.* (1983). (*b*) Perspective view of one stacking unit.

Ising) model, in an approach similar to that employed by Price *et al.* (1985) to compute a stacking fault energy in a magnesium silicate spinelloid. The ANNNI model is a statistical mechanics model, originally developed to describe magnetic systems. It was adapted to describe polytypism in minerals by Smith *et al.* (1984), and Price and Yeomans (1984) by mapping the basic polytypic structural unit on to a magnetic spin variable. The interactions between units can then be written as a Hamiltonian with competing interactions to form a model which provides a simple equilibrium description of polytypism, and, using short-range couplings, can predict the stable polytypes for a given compound.

The internal energy of a particular structure is assumed to be made of two components: (i) the internal energy of component modules, and (ii) the energy of interaction between modules. If the internal energy of the components is invariant, the difference in calculated lattice energies will reflect the difference in the interaction energy between modules. In this study of $MgSiO_3$ perovskite, the interaction energy between the first four neighbouring modules only is considered.

The ground state energy for the normal stacking sequence of $MgSiO_3$ perovskite per N layers is:

$$E\langle 1\rangle = NJ_1 + NJ_3 + NE_\infty$$

(see Price *et al.*, 1985, for the derivation) where J_1 and J_3 are interaction energies between the first and third neighbours having the opposite sense ($\uparrow\downarrow$), and E_∞ the lattice energy of the $\langle\infty\rangle$ structure. The introduction of a stacking fault on {110} changes this to:

$$E\langle 1\rangle^* = (N-1)J_1 + 2J_2 + (N-3)J_3 + 4J_4 + NE_\infty$$

where J_2 and J_4 are the interaction energies between the second and fourth neighbours which have the opposite sense and are created by the introduction of the stacking fault. The energy of the stacking fault is, therefore:

$$E\langle\text{fault}\rangle = -1J_1 + 2J_2 - 3J_3 + 4J_4.$$

The interaction energies J_1, J_2, J_3, J_4, have been evaluated by calculating the lattice energies of hypothetical structures with stacking sequences $\langle 1\rangle$, $\langle 2\rangle$, $\langle 21\rangle$, $\langle 31\rangle$, and $\langle 3\rangle$. These calculations have been made at simulated pressures of 0, 100, 500, 1000, and 2000 kbars using potentials W2 and W3. As we would expect, the cubic phase $\langle 1\rangle$ is the most stable at all the pressures considered.

The stacking fault energy at 0 kbars has been calculated to be 1.67 J m^{-2} using W2 and 1.95 J m^{-2} using W3. The stacking fault energy increases with increasing pressure (see Table V), and by 1000 kbars it is 2.52 J m^{-2} (W2) and 3.24 J m^{-2} (W3). The stacking fault energy provides a measure of the equilibrium distance of separation (d) between the two partial dislocations bounding the stacking fault, which can be found using the relationship $d = \mu(b_2 \cdot b_3 \cos\theta)/(2 \cdot \pi \cdot \gamma)$ (Hull, 1975) where μ is the shear modulus, b_2 and b_3 are the Burgers vectors of the partial dislocations, θ the angle between them, and γ the stacking fault energy. The distance of separation, d, at 1 bar is 8.37 Å or 1.7 b_1, (where b_1 is the full Burgers vector), using W2 and 8.41 Å or 1.7 b_1 using W3. By 1 Mbar this distance is predicted to increase to 11.5 Å or 2.6 b_1 (W2), and 9.24 Å or 2b_1 (W3). The distance of separation has increased by 1 Mbar because the shear modulus, μ, increases by a factor of 3 using W2 or 2.5 using W3, whereas the stacking fault energy only increases by a factor of 1.7 (W2) and 1.5 (W3). At 1 bar the value of the stacking fault energy in $MgSiO_3$ perovskite is two orders of magnitude greater than in magnesium silicate spinelloids (Price *et al.*, 1985) and, conversely, the distance of separation of the partial dislocations is two orders of magnitude less.

Table V Stacking fault energies (Jm^{-2}).

P(kbar)	0	100	500	1000	2000
W2	1.67	1.80	2.23	2.52	2.90
W3	1.95	2.08	2.47	2.81	3.24

The calculated stacking fault energy is, therefore, high, and the distance of separation of the partial dislocations small, suggesting that any dislocations of the type [110] will tend not to dissociate greatly and hence will not have enhanced mobility. The small increase in separation with pressure is unlikely to influence greatly the ease with which this glide system can operate at high pressures.

Conclusions

The structure of $MgSiO_3$ perovskite at 1 bar has been successfully simulated using potentials W1, W2, and W3 which were derived by fitting to the experimentally derived structural data. However, potentials W4 and N1, which include terms transferred from other compounds, did not reproduce the structure quite so well. The elastic properties are more difficult to simulate, but good results were obtained using potential W3 which was also fitted to the bulk and shear moduli and the high-frequency dielectric constant.

Potentials W1, W2, and W3 were used to investigate the possible phase changes between the orthorhombic, hypothetical cubic and tetragonal

perovskite polymorphs. A comparison of the free energies of the simulated orthorhombic and ideal cubic perovskite polymorphs, calculated using W2 and W3, leads to the prediction that the orthorhombic phase is stable at all but the highest pressures. With increasing pressure these potentials also simulate a decrease in the degree of orthorhombic distortion, shown by unit cell ratios closer to those of the cubic perovskite and a decrease in the angle of rotation of the SiO_6 octahedra. Therefore, we propose that the temperature of the orthorhombic to cubic perovskite transition may decrease with increasing pressure. However, when potential W1 is used, the orthorhombic phase is always predicted to be the more stable. All three potentials predict that, should they exist, a phase change would occur between the tetragonal and cubic perovskite polymorphs with increasing pressure.

Changes in the structure of orthorhombic perovskite in response to increasing pressure (i.e. whether the orthorhombic distortion increases or decreases) are probably dependent on the relative compressibilities of the SiO_6 and MgO_{12} polyhedra. We suggest that it is important to consider, at least, the shortest 8 bonds in the MgO_{12} polyhedron because the shorter bonds are much less compressible than the longer ones. The change in distortion of the orthorhombic perovskite, measured by φ, the angle of rotation of the SiO_6 octahedra about their threefold axes, may depend on the total perovskite bulk modulus (K_{pv}) and the SiO_6 octahedron bulk modulus (K_{SiO_6}) such that $d\varphi/dP = \frac{1}{2}\cot\varphi(1/K_{pv} - 1/K_{SiO_6})$. The change in distortion will decrease if K_{pv} is larger than K_{SiO_6} as is simulated to be the case at high pressure using potentials W2 and W3.

The relative stabilities of perovskite polytypes containing hexagonally close packed as well as cubic close packed layers, based on the structures of the ideal cubic perovskite, the hexagonal perovskite $BaNiO_3$, high $BaMnO_3$, and hexagonal $BaTiO_3$ were investigated at pressures up to 2 Mbar. The ideal cubic perovskite was found to have the most stable structure. The energy of a stacking fault on (110), as proposed by Poirier *et al.* (1983), was estimated using the ANNNI model (Price *et al.*, 1985) to be between 1.67 J m^{-2} and 1.95 J m^{-2} depending on the interatomic potential used. The stacking fault energy is predicted to increase with increasing pressure, but the separation distance of the partial dislocations actually increases from 8.4 to 11.5 Å (or 8.4 to 9.2 Å) because of the greater increase in the shear modulus.

These potentials, particularly W3, may now be used in other computer codes which simulate, for example, phonon frequencies and defect energies, as well as in molecular dynamics programs that include the effect of temperatures above absolute zero. It may also be desirable to develop further potentials which include three body terms to take into account the angular relationships between O–Si–O in the SiO_6 octahedron. We believe that the progress reported in this paper will enable us to investigate the further properties of $MgSiO_3$ perovskite which determine the behaviour of the Earth's mantle and the dynamics of plate tectonics.

Acknowledgements. We would like to thank W. R. Busing and C. R. A. Catlow for the programs WMIN and METAPOCS, J. R. Baker for drafting the figures, and M. J. Mendelssohn for the PLUTO plotting program. AW gratefully acknowledges receipt of a NERC studentship and GDP receipt of a Royal Society Research Fellowship and NATO research grant 828/83.

REFERENCES

Bass, J. D. (1984) Elasticity of single-crystal $SmAlO_3$, $GdAlO_3$, and $ScAlO_3$ perovskites. *Phys. Earth Planet. Inter.* **36,** 145–56.

Burnham, C. W. (1985) Mineral structure energetics and modelling using the ionic approach. *Reviews in Mineralogy*, **14.** (S. W. Kieffer and A. Natrotsky, eds.). Mineral. Soc. America, 347–88.

Busing, W. R. (1981) *WMIN, a computer program to model molecules and crystals in terms of potential energy functions.* Oak Ridge National Laboratory, Oak Ridge, Tennessee.

Catlow, C. R. A. (1977) Point defects and electronic properties of uranium dioxide. *Proc. R. Soc. London,* **A353,** 533–61.

—— and Mackrodt, W. C. (1982) Computer simulation in solids. *Lecture notes in physics*, **166.** Springer, Berlin.

——Cormack, A. N., and Theobald, F. (1984) Structure prediction of transition metal oxides using Energy minimization Techniques. *Acta Crystallogr.* **B40,** 195–20.

Clarke, R., and Benguigui, L. (1977) The tricritical point in $BaTiO_3$. *J. Phys. C: Solid State Phys.* **10,** 1963–73.

Dziewonski, A. M., and Anderson, D. L. (1981) Preliminary reference earth model. *Phys. Earth Planet. Inter.* **25,** 297–356.

Fisher, M. E., and Selke, W. (1981) Low temperature analysis of the axial next-nearest neighbour Ising model. *Phil. Trans. R. Soc.* **302,** 1–44.

Glazer, A. M. (1975) Simple ways of determining perovskite structures. *Acta Crystallogr.* **A31,** 756–62.

Granicher, H., and Jakits, O. (1954) Uber die dielektischen Eigenschaften und Phasenumwandlungen bei Mischkristallsystemen vom Perowskittyp. *Nuovo Cimento*, **9,** Suppl. 10, 480–520.

Hazen, R. M., and Finger, L. W. (1982) *Comparative Crystal Chemistry.* Wiley, New York.

Hull, D. (1975) *Introduction to dislocations.* Pergamon Press Ltd. Oxford.

Ikeda, T. (1975) Effect of hydrostatic pressure on the phase transition of ferroelectric $PbTiO_3$. *Solid State Comm.* **16,** 103–4.

Ito, E., and Matsui, Y. (1978) Synthesis and crystal-chemical characterization of $MgSiO_3$ perovskite. *Earth Planet. Sci. Lett.* **38,** 443–50.

Kittel, C. (1976) *Introduction to solid state physics.* John Wiley and Sons, New York.

Knittle, E. Jeanloz, R., and Smith, G. L. (1986) Thermal expansion of silicate perovskite and stratification of the Earth's mantle. *Nature,* **319,** 214–15.

Lieberman, R. C., Jones, L. E. A., and Ringwood, A. E. (1977) Elasticity of aluminate, titanate, stannate and germate compounds with the perovskite structure. *Phys. Earth Planet. Inter.* **14,** 165–78.

Liu, L. (1976) The high pressure phases of $MgSiO_3$. *Earth Planet. Sci. Lett.* **31,** 200.

Mandarino, J. A. (1976) The Gladstone–Dale relationship—Part I: Derivation of new constants. *Can. Mineral.* **14,** 498–502.

——(1978) The Gladstone–Dale relationship—Part II: Trends among constants. Ibid. **16,** 169–74.

——(1979) The Gladstone–Dale relationship—Part III: Some general applications. Ibid. **17,** 71–6.

Martin, G., and Hegenbarth, E. (1973) The influence of hydrostatic pressure on the ferroelectric phase transition of $CdTiO_3$ ceramics. *Phys. Stat. Sol.* (a) **18,** K151-2.

Megaw, H. D. (1973) *Crystal Structures: a working approach.* Studies on physics and chemistry no. 10. W. B. Saunders Co., Philadelphia, London, Toronto.

Miyamoto, M., and Takeda, H. (1984) An attempt to simulate high pressure structures of Mg-silicates by an energy minimization method. *Am. Mineral.* **69,** 711–18.

Muller, O., and Roy, R. (1974) *The major ternary structural families.* Springer, Berlin.

Okai, B., and Yoshimoto, J. (1975) Pressure dependence of the structural phase transition temperature in $SrTiO_3$ and $KMnF_3$. *J. Phys. Soc. Japan,* **39,** 162–5.

O'Keeffe, M., and Bovin, J. (1979) Solid electrolyte behavior of $NaMgF_3$: geophysical implications. *Science,* **206,** 599–600.

——Hyde, B. G., and Bovin, J. (1979) Contribution to the crystal chemistry of orthorhombic perovskites: $MgSiO_3$ and $NaMgF_3$. *Phys. Chem. Minerals,* **4,** 299–305.

Parker, S. C. (1983*a*). Prediction of mineral crystal structures. *Solid State Ionics,* **8,** 179–86.

——(1983*b*) Ph.D. thesis, University of London.

——Catlow, C. R. A., and Cormack, A. N. (1984) Structure prediction of silicate minerals using energy-minimization techniques. *Acta Crystallogr.* **B40,** 200–8.

Poirier, J. P., Peyronneau, J., Gesland, J. Y., and Brebac, G. (1983) Viscosity and conductivity of the lower mantle; an experimental study on a $MgSiO_3$ perovskite analogue, $KZnF_3$. *Phys. Earth Planet. Inter.* **32,** 273–87.

Prewitt, C. T. (1985) Crystal chemistry: past, present, and future. *Am. Mineral.* **70,** 443–54.

Price, G. D., and Parker, S. C. (1984) Computer simulation of the structural and physical properties of the olivine and spinel polymorphs of $MgSiO_3$. *Phys. Chem. Minerals,* **10,** 209–16.

——and Yeomans, J. (1984) The application of the ANNNI model to polytypic behaviour. *Acta Crystallogr.* **B40,** 448–54.

—— Parker, S. C., and Yeomans, J. (1985) The energetics of polytypic structures: a computer simulation of magnesium silicate spinelloids. Ibid. **B41,** 231–9.

Samara, G. A. (1970) Pressure and temperature dependence of the dielectric properties and phase transitions of the antiferroelectric perovskites: $PbZrO_3$ and $PbHfO_3$. *Phys. Review,* **B1,** 3777–86.

——(1971) Pressure and temperature dependence of the dielectric properties and phase transitions of the ferroelectric perovskites: $PbTiO_3$ and $BaTiO_3$. *Ferroelectrics,* **2,** 277–89.

Smith, J., Yeomans, J., and Heine, V. (1984) In *Proceedings of NATO Advanced Studies Institute on modulated structure materials.* (T. Tsakalakos, ed.). Dordrecht: Nijhoff, 95.

Swanson, D. K., and Prewitt, C. T. (1983) The crystal structure of $K_2Si^{VI}Si_3^{IV}O_9$. *Am. Mineral.* **68,** 581–5.

Yagi, T., Mao, H., and Bell, P. M. (1978) Structure and crystal chemistry of perovskite-type $MgSiO_3$. *Phys. Chem. Minerals,* **3,** 97–110.

————(1982) Hydrostatic compression of perovskite-type $MgSiO_3$. In *Advances in Physical Geochemistry,* **2** (S. K. Saxena, ed.). Springer-Verlag, New York, 317–27.

[*Manuscript received 2 October 1985; revised 7 February 1986*]